

Document downloaded from:

<http://hdl.handle.net/10251/65702>

This paper must be cited as:

Carenco, S.; Leyva Perez, A.; Concepción Heydorn, P.; Boissiere, C.; Mezailles, N.; Sanchez, C.; Corma Canós, A. (2012). Nickel phosphide nanocatalysts for the chemoselective hydrogenation of alkynes. *Nano Today*. 7:21-28.
doi:10.1016/j.nantod.2011.12.003.



The final publication is available at

<https://dx.doi.org/10.1016/j.nantod.2011.12.003>

Copyright Elsevier

Additional Information

Nickel phosphide nanocatalysts for the chemoselective hydrogenation of alkynes

Sophie Carenco,^{1,2} Antonio Leyva-Pérez,³ (Patricia Concepción,³ ?) Cédric Boissière,¹ Nicolas Mézailles,^{2,} Clément Sanchez,^{1,*} Avelino Corma^{3,*}*

¹Laboratoire de Chimie de la Matière Condensée, Collège de France, UPMC, CNRS, Paris, France;

²Laboratoire Hétéroéléments et Coordination, Ecole Polytechnique, CNRS, Palaiseau, France ; ³Instituto de Tecnología Química, Universidad Politécnica de Valencia-Consejo Superior de Investigaciones Científicas, Valencia, Spain.

E-mail: nicolas.mezailles@polytechnique.edu, clement.sanchez@upmc.fr, acorma@itq.upv.es

Well-defined 25 nm nickel phosphide nanoparticles act as a colloidal catalyst for the chemoselective hydrogenation of terminal and internal alkynes. *Cis*-alkenes are obtained in mild conditions (85°C, a few hours) with good conversion and selectivity. The phosphorus inserted in the Ni-P nanoparticles is critical for the selectivity of the nanocatalyst. Mechanistic investigations support a pre-reduction of the catalyst for its activation. They pinpoint the occurrence of C-H bond cleavage in terminal alkynes during the reaction.

1. Introduction

The selective hydrogenation of alkyne to alkene is a major industrial reaction that has relevant applications in fields such as polymerization (removal of phenylacetylene in the styrene feedstocks)¹ and fine chemical synthesis. As a cheaper and greener alternative to the traditional Pd-based Lindlar catalysts, nickel-based heterogeneous catalysts have been developed, such as Raney Nickel. However,

they show a lack of selectivity and yield mixtures of alkenes and alkanes, as they can also hydrogenate olefins.^{2,3,4,5}

In the early 1980's, it was shown that phosphorus-containing nickel catalysts exhibited attenuated hydrogenation activities due to the electronic withdrawing effect of the phosphorus on the nickel.⁶ A wide variety of Ni-P structures have been obtained, with stoichiometry ranging from Ni₃P to NiP₃.⁷ They feature oxidation states and electronic properties that strongly depend on the Ni/P ratio.⁸ The Ni-rich phosphides, having a metallic character,⁹ have been used as heterogeneous catalysts. Besides its early use for the reduction of nitrobenzene,¹⁰ this family of catalysts was almost exclusively (but extensively) developed in the field of feedstocks hydrotreating, with significant successes.¹¹ Among the Ni-rich phases (Ni₃P, Ni₁₂P₅, Ni₅P₄, Ni₂P), the Ni₂P phase have been studied the most, as it is highly stable, in particular upon sulfur exposure, which makes it very efficient in hydrodesulfurization processes.¹²

Interestingly, T. Oyama and co-workers demonstrated that the Ni₂P surface catalyzes the hydrodesulfurization of the most difficult substrate, namely the sterically hindered 4,6-dimethyldibenzothiophene, through an hydrogenation route that involves selectively one of the two nickel sites in the hexagonal Ni₂P lattice.¹³ This hydrogenation is usually disfavored over the direct desulfurization for other substrates. In this study, the experimental conditions were quite harsh (31 bar, 340°C) yet in the typical range of the studies dealing with Ni-P heterogeneous catalysts. From an external point of view, it pinpoints that Ni₂P could be a suitable catalyst for classical hydrogenation reactions of more reactive substrates, in milder conditions. Very recently, it was shown that TiO₂-promoted or CeO₂-promoted bulk Ni₂P hydrogenated the phenylacetylene in styrene and ethylbenzene in softer conditions (150°C, 10 bars).¹⁴ While the selectivity for this simple substrate is interesting (up to 90% selectivity for styrene), the operating conditions (high temperature, high pressure) precludes their use for fine chemicals transformations.

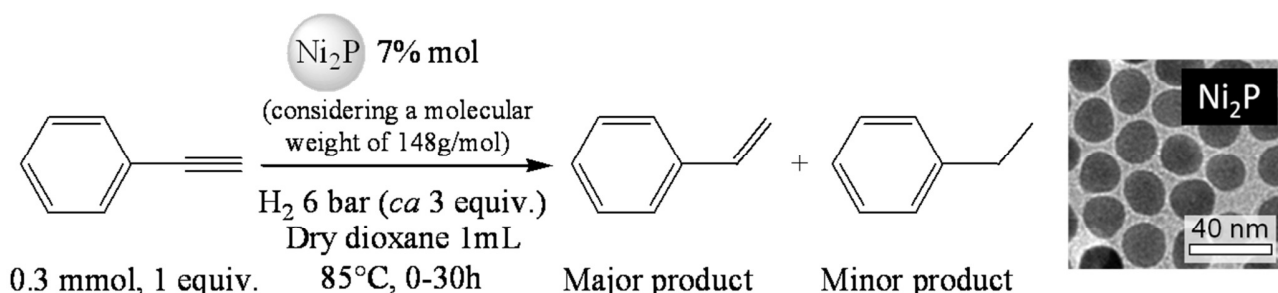
In the present work, the activity and selectivity of well-defined Ni₂P nanoparticles as a colloidal solution are investigated in the hydrogenation of alkynes for a wide range of substrates, in very mild

conditions (85°C, 6 bar of H₂) that are compatible with the presence of various functional groups. High conversions of various alkynes are obtained in a few hours with a very good selectivity (up to 100%) and a wide functional group tolerance. A mechanistic study provides new insights on the roots of the selectivity for the *cis*-alkene derivatives.

2. Results and discussion

2.1 Hydrogenation of phenylacetylene

The hydrogenation of a model alkyne, phenylacetylene, was achieved under mild conditions in a batch reactor using well-defined Ni₂P nanoparticles. The spherical, monodispersed in size (25 nm diameter) and fully crystallized Ni₂P nanoparticles were obtained by reacting Ni monodispersed nanoparticles with 1/8 P₄, in a fully reproducible and gram-scale synthesis (see ESI).¹⁵ Reaction conditions for the catalysis experiments are described in Scheme 1 and in the experimental section.



Scheme 1: Reaction conditions for the hydrogenation of phenylacetylene catalyzed by Ni₂P nanoparticles (see Experimental Section for the details)

Figure 1 shows that phenylacetylene conversion of 98% was reached in 6 h, with a very good selectivity for styrene (96%). From this first set of observations, it appears that the Ni₂P catalyst hydrogenates more easily the alkyne function than the alkene one. This feature results in a two step reaction where all the alkyne was hydrogenated (1 to 20 h) before the alkene started to convert into alkane. Hence, a high selectivity for the alkene can be easily managed.

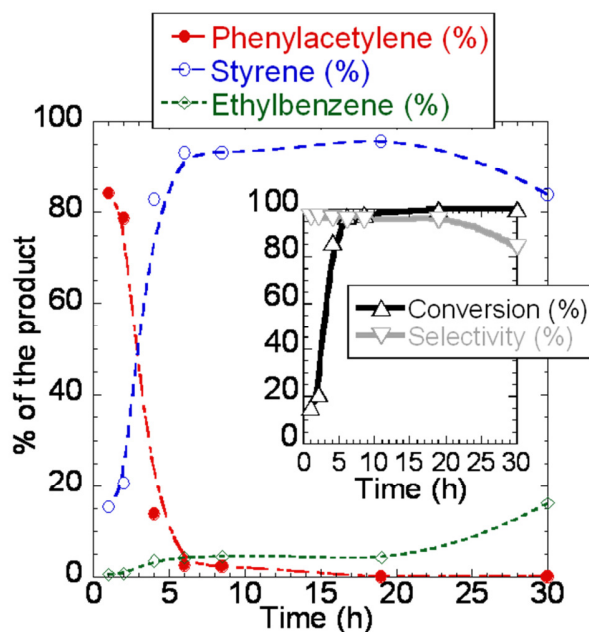


Figure 1: Hydrogenation of phenylacetylene catalyzed by Ni₂P nanoparticles. Main graph: composition of the reaction mixture at different times. Insert: Corresponding conversion of phenylacetylene and selectivity for styrene. The lines are a guide to the eye.

Recent studies pinpoint that leaching of the nanoparticles can be responsible for the catalytic activity of nanoparticles.¹⁶ In order to rule out this possibility here, a filtration test was done: the reaction was stopped after 4 h at a conversion of 83%, the H₂ pressure was released and the nanoparticles were removed. Then, the corresponding filtrate was heated back to 85°C under 6 bar of fresh H₂. No evolution of the composition mixture was observed in the following hours, indicating that the Ni₂P nanoparticles were responsible for the catalytic activity.

As a confirmation of the integrity of the catalyst after the reaction, TEM and XRD analyses of the spent catalyst presented no difference with the starting nanoparticles (see ESI).

2.2 Scope of the reaction

This high selectivity for single hydrogenation process was observed for a variety of aryl- and also alkyl-terminal alkynes (Table 1). The reaction was found to be tolerant to various functional groups including halides (entries 1 and 2), alcohols (entry 3) and amines (entry 4). In order to further examine the alkyne-to-alkene selectivity, four different enyne substrates were prepared and tested. Firstly, a

terminal aryl alkyne was selectively hydrogenated to the corresponding styrene derivative in the presence of an internal *trans*-alkene in high yield (entry 5). The same satisfactory result was obtained when an alkyl counterpart is used (entry 6). If the positions of the alkyne and alkene moieties are interchanged in the molecule, a good selectivity was still found, although the yield dropped significantly (entry 7). It must be noted that internal alkynes are 100 times less reactive than terminal alkenes in related reactions.¹⁷ Therefore, the last result illustrates the high selectivity of the Ni₂P nanocatalyst towards alkynes *vs.* alkene. Finally, a retinol derivative containing a conjugated π -system of five alkenes with a single terminal alkyne was hydrogenated to give a reasonable 30% yield of the all-alkenyl compound (entry 8). In contrast, the introduction of nitro groups dramatically reduced the hydrogenation of the alkyne (entry 9), first because of its electron withdrawing effect on this particular alkyne, second because it competes with the alkyne as a substrate of the hydrogenation reaction, yielding the corresponding amino derivative.¹⁸

As mentioned above, internal alkynes are less prone to hydrogenation due to steric reasons. However, with Ni₂P as a nanocatalyst, internal alkynes could also be hydrogenated selectively in the corresponding *cis*-alkene (entries 10-14). The conversion remained good for alkynes with a limited steric hinderance (entry 10-11), while more hindered alkynes reacted poorly, but always with a good selectivity for the alkene (entries 12-14). The reaction was also much slower in the presence of a terminal carboxylic acid (entry 11), which again points out that a strong coordination of one side of the molecule to the surface disfavored the alkyne reaction. On the contrary, a comparison between entries 12 and 13 underlines that the amine moiety in the vicinity of the alkyne may favor the hydrogenation (although the amine in ortho position also acts as an activating group). Finally, an internal aryldiyne was doubly hydrogenated tot the diene, with a lower yet reasonable selectivity (entry 15).


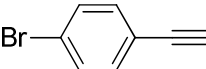
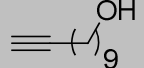
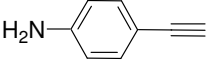
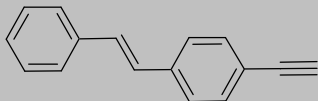
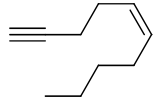
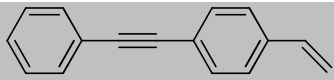
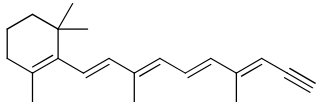
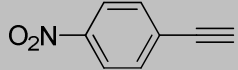
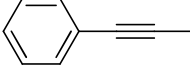
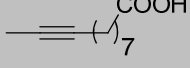
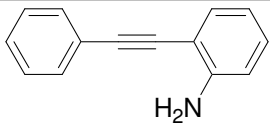
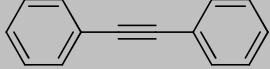
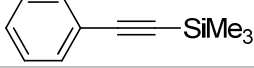
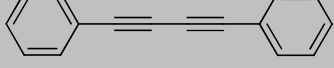
| Entry | Alkyne | Conv. | Alkene | Alkane | Selectivity | Time | Comments |
|-------|---|-------|---------------------|--------|-------------|------|---|
| 1 |  | 95% | 95% | 0% | 100% | 14h | The halide function does not react. |
| 2 |  | 75% | 72% | 3% | 96% | 14h | The halide function does not react. |
| 3 |  | 75% | 60% | 15% | 80% | 14h | (i) |
| 4 |  | 31% | 24% | 7% | 78% | 14h | |
| 5 |  | 80% | 76% | 0% | 95% | 14h | 4% internal alkene hydrogenated. (i) |
| 6 |  | 54% | 46% | 4% | 85% | 14h | 4% internal alkene hydrogenated |
| 7 |  | 28% | 23% cis 5% trans | 0% | 82% | 60h | Competitive hydrogenation of the terminal alkene: 26% |
| 8 |  | 90% | 30% | 60% | 33% | 14h | (i), (a) |
| 9 |  | 7% | 3% | 0% | 43% | 14h | Formation of 4% of amino-phenylacetylene. |
| 10 |  | 71% | 63% cis 4% trans | 3% | 89% | 14h | |
| 11 |  | 82% | 76% All cis | 6% | 93% | 48h | (i), (b) |
| 12 |  | 19% | 19% cis | 0% | 100% | 18h | |
| 13 |  | 9% | 9% cis | 0% | 100% | 18h | |
| 14 |  | 3% | 3% cis | 0% | 100% | 18h | |
| 15 |  | 88% | 52% | 36% | 59% | 18h | (i), (ii), (c) |

Table 1: Scope of the reaction. *Notes:* (i) Product isolated, mass balance 100%. (ii) The alkene yield corresponds to diene (no enyne). The alkane yield sums the fully hydrogenated product and the monoalkenes. *Specific conditions:* (a) substrate (0.07 mmol), dioxane (0.12 mL), 0.1 equiv of Ni₂P, 2 bar of H₂, 85°C. (b) Catalyst: 0.2 equiv. (c) 0.4 equiv. of catalyst (0.2 equiv. per triple bond).

Altogether, the Ni₂P nanoparticles catalyst exhibit an interesting selectivity, combined with good conversions, for the hydrogenation of elaborated substrates. Note that the very good *cis*-selectivity correlates well with a hydrogenation that occurs on the surface of the nanoparticles and not with leached species. The presence of small amounts of trans-alkene may be due to a secondary isomerization mechanism in the reaction mixture.

2.3 Recyclability of the catalyst

Nanoparticles catalysts can easily be separated from the reaction mixture in order to be recycled. In this purpose, phenylacetylene was chosen as the substrate and the reaction was stopped after 6 h. The nanoparticles were separated by centrifugation and reused in two additional runs of 6 h. A small drop was observed in terms of selectivity, but the overall conversion remained very high (Figure 2), even higher than with the starting sample. This latter point is related to the activation of the nanocatalyst and will be discussed later.

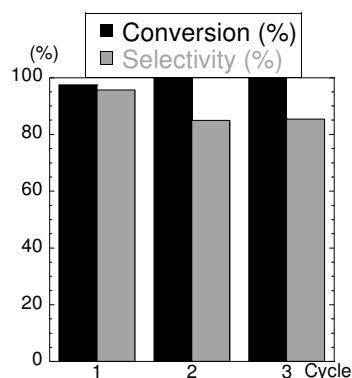


Figure 2: Recycling of the Ni₂P catalysts for the hydrogenation of phenylacetylene.

2.4 Mechanistic insights

Isotopic Experiments

The hydrogenation of alkyne on the nanoparticles surface involves at least two main steps: (i) H₂ dissociation to yield surface hydride, (ii) alkyne coordination on the surface. In order to gain information about the limiting step of the reaction, the hydrogenation of *D*-phenylacetylene (the deuterium is on the terminal *sp* carbon) was monitored over time. Both sets of data (*H*-phenylacetylene and *D*-phenylacetylene hydrogenations) are plotted on Figure 3. They feature a similar induction time of

2 h and thus, the initial rates were estimated after 2 h of reaction. A kinetic isotope effect of 2.4 was observed, which highlighted that the phenylacetylene substrate is involved in the limiting step of the reaction.

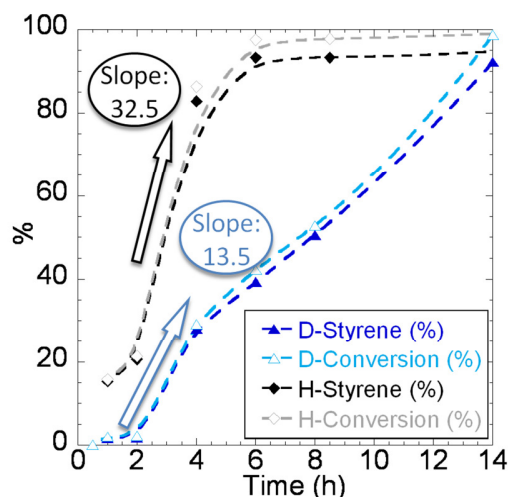
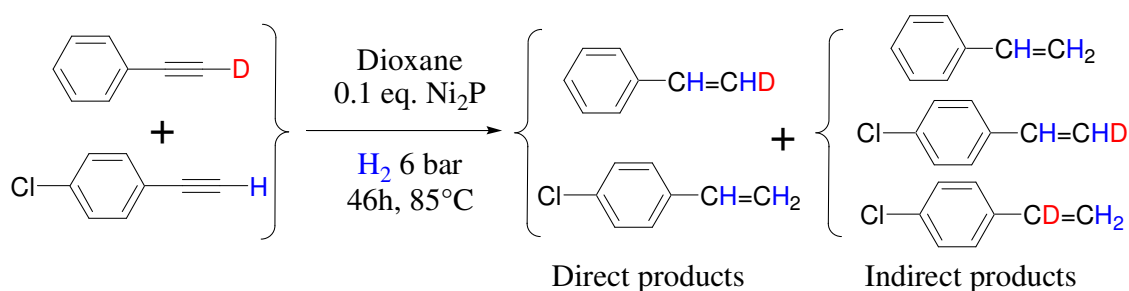


Figure 3: Conversion and styrene yield over time for H-phenylacetylene and D-phenylacetylene. The lines are a guide to the eye.

In terms of mechanism, this result suggested that C-H activation occurred on the surface of the catalyst, leading to the formation of hydride species. Thus the terminal H of the alkyne could become an active hydride species during the reaction. In order to test this hypothesis, cross-reactions involving two different alkynes (*D*-phenylacetylene and *p*-chlorophenylacetylene) were performed (Scheme 2). The duration of the reaction was chosen to be long enough (46 h) to yield full conversion of the two alkynes.



Scheme 2: Cross-reaction between deuterated and non-deuterated alkynes. If no C-D bond breaking is involved, the indirect products should not be observed. On the opposite case, they should form as minor products.

The analysis of the final mixture showed the presence of significant amounts of chloro-derivatives that were labeled with D (see ESI). This observation thus confirmed that the breaking of the C-H/C-D bond of the terminal alkyne occurred on the surface of the nanoparticles.

Induction Period

As noted above, the hydrogenation of phenylacetylene exhibits an induction period of *ca* 2 h. This delay seems to diminish significantly when using recycled nanoparticles. We believe that this induction time has a double cause: (i) the surface of the nanoparticles need to be reduced by H₂ to produce the active catalyst species (chemical reactivity), and/or (ii) the surface of the nanoparticles is not accessible to the substrate as the starting powder needs to be disaggregated (colloids dispersion) and/or the phosphine ligands that cover the nanoparticles¹⁹ need to make room for the alkyne moiety through an exchange process (chemical availability). Indeed, complementary experiments were run by introducing sequentially H₂ and the alkyne (H₂ first of the alkyne first) with an interval of 2h. Both experiments showed the same induction time behavior than before, meaning that neither preliminary reductive conditions, neither preliminary stirring, promoting ligand displacement by the alkyne, can suppress the induction period.

In situ spectroscopic experiments (XPS or other) would be mandatory to completely characterize the active species of the catalyst: they are beyond the scope of this study. Rather, the emphasis was put here on the tailoring of the starting Ni/P ratio (see below).

XPS or H/D exchange results could be inserted here in a dedicated section concerning the surface state.

2.5 Influence of the Phosphorus loading in the nanoparticles on the selectivity of the catalyst

The role of phosphorus in the metal phosphide structure can be assessed by varying “manually” the Ni/P ratio and comparing the corresponding catalytic activity, keeping all the other parameters constant: nanoparticles mean size, ligands sets, etc. Pure-Ni nanoparticles and Ni_{3.5}P nanoparticles were then compared with Ni₂P nanoparticles for the hydrogenation of phenylacetylene. One should note that the so-called Ni_{3.5}P nanoparticles exhibit in fact a core-shell structure: a Ni₂P monocrystallized core surrounded by a 2 nm polycrystallized shell of Ni (Figure 4, left), as described in a previous work.²⁰

The hydrogenation of phenylacetylene was faster for the new catalysts than for Ni₂P, mainly because the induction period disappeared with both samples (see Figure 4, Middle inset). This fact tends to confirm that the induction time for Ni₂P corresponds to the formation of “true” Ni(0) species on the surface. Besides this effect, the initial rate is in the same range. However, the Ni/P ratio strongly impacts the selectivity of the reaction. Using Nickel nanoparticles, the styrene is quickly hydrogenated to ethylbenzene. This secondary process is slower with Ni_{3.5}P, which exhibit an intermediate behavior between Ni and Ni₂P. Finally, an acceptable chemoselectivity is found only when Ni₂P nanoparticles are used as catalyst (Figure 4, right).

Several hypotheses could explain the behavior of the core-shell Ni_{3.5}P nanoparticles: (i) an electronic effect of the core on the shell that disfavor the alkene hydrogenation, (ii) a crystallographic effect: the small Ni crystallite of the shell cannot hydrogenate alkene, (iii) a redistribution effect; at 85°C, the structure may reorganize to an amorphous and homogeneous Ni-P solid solution. Hypothesis (i) seems fragile because there is no electronic effect of the core on the rate of alkyne conversion in the first minutes (Figure 4, Middle inset). About (ii), one should remember that the Ni nanoparticles are not monocrystallized either, but result of the aggregation of 5 nm crystallites. Thus, they also contain many defects: this weakens the whole hypothesis. (iii) is compatible with several observations that point out an increased atomic mobility in small nanoparticles at moderate temperatures.²¹ Indeed, Ni_{3.5}P nanoparticles behave like nickel in the first minutes but then turn out to have a mixed behavior at longer reaction times, which fits with the redistribution effect hypothesis. Altogether, the presence of phosphorus clearly improves the selectivity of the catalyst. One could consider that it acts as a “poison”, which is reminiscent of the case of highly selective Pd-poisoned catalyst.

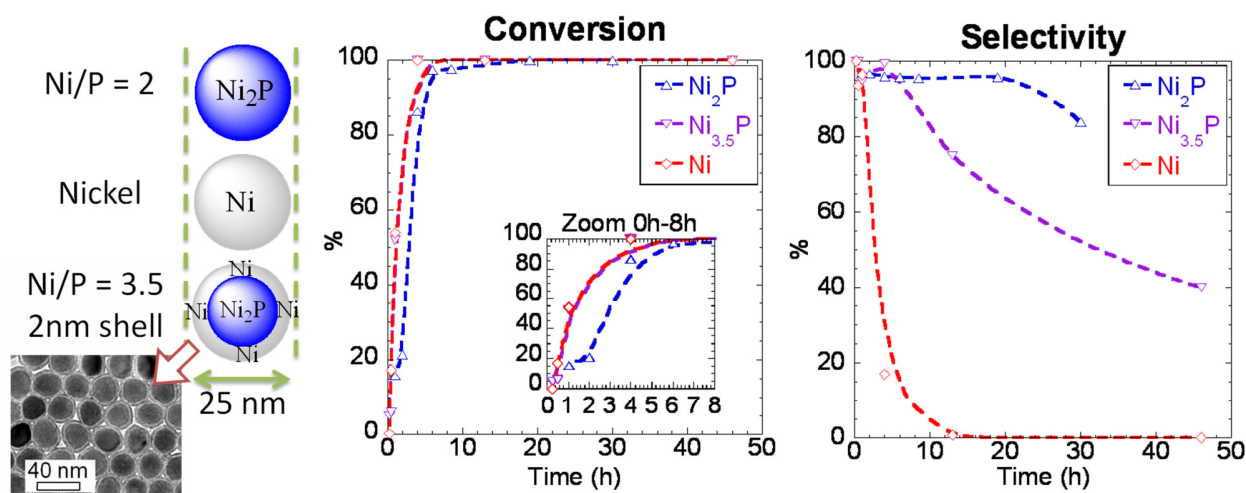


Figure 4: (Left) Schematic structures of the nanoparticles, and a TEM pictures of the core-shell Ni_{3.5}P nanoparticles; (Middle and Right) Conversion and selectivity obtained with Ni₂P, Ni_{3.5}P and Ni nanoparticles. The lines are a guide to the eye.

In this work, the relevance of nickel phosphide as a cheap catalyst for the selective hydrogenation of alkyne to *cis*-alkene was demonstrated for a wide variety of substrates. Nanoscaling of the catalyst provided a high surface/volume ratio, which favored good activities in mild conditions of temperature (85°C) and pressure (6 bars), compared with typical heterogeneous conditions (several hundreds of degrees and a higher pressure). The choice of a colloidal catalyst required dealing with the surface ligands, which were at least partially responsible for an initial low reaction rate, but it presented the advantage of being compatible with complex organic substrates manipulation, in contrast with high-temperature flow processes. Mechanistic investigations also pointed out the necessity to activate the nanocatalyst by H₂ reduction, and showed that the presence of the alkyne from the beginning of the reaction also played a role in the catalyst activation. Concerning the design of the nanoparticles, phosphorus loading in the nickel phosphide nanoparticles was shown to be critical for the selectivity of the catalyst. Further studies on these monodispersed nanoparticles could lead to a correlation between the mean diameter and the rate of reaction. Moreover, cross-reactions involving a deuterated alkyne highlighted that C-H insertion occurs in the terminal alkyne, which opens the door to C-C and C-H heteroatom coupling reactions. Altogether, the metal phosphide family, which deeply contributed to the

design of heterogeneous hydrotreating robust and active catalysts, could now bring interesting perspectives to fine chemical synthesis and to homogeneous catalysis in general.

3. Experimental Section

3.1 Catalysis setup

A typical reaction of hydrogenation was performed as follow: In a 3mL glass reactor equipped with a manometer and washed with aqua regia before use, 1 mL of dry dioxane was added. 0.07 equiv. of Ni₂P nanoparticles were added (0.02 mmol, 3.0 mg, the stoichiometry is based on the molecular formula “Ni₂P”, M=148 g/mol), along with 1 equiv. of phenylacetylene (0.3 mmol, 30.6 mg, 32.9 μL). The air was purged and 6 bar of H₂ were added (corresponding to *ca* 3 equiv.). The reactor was heated at 85°C in an oil bath and stirred during the reaction. For the reaction involving Ni nanoparticles and Ni_{3,5}P nanoparticles, the comparison was done by keeping the number of Ni mole constant (*i.e.* 0.04 mmol of Ni). At the end of the reaction, the pressure was released, and the composition of the mixture was analyzed by GC-MS.

3.2 Substrates synthesis

Undec-5-en-1-yne²² (Table 1, entry 6), *p*-(1-phenylethynyl)styrene²³ (entry 7) and 2-(phenylethynyl)aniline²⁴ (entry 12) were prepared according to reported procedures.

***p*-(1*E*-Styryl)phenylacetylene (Table 1, entry 5).** Dimethyl-1-diazo-2-oxopropylphosphonate (Ohira-Bestmann reagent, 1.149 g, 6.0 mmol) and K₂CO₃ (1.38 g, 10 mmol) were placed in a 100 ml round-bottomed flask and two vacuum-nitrogen cycles were done, leaving a nitrogen atmosphere finally by sealing with a rubber septum and injecting a balloon with nitrogen. Dry methanol (40 ml) was added and then a dispersion of *p*-(1-styryl)benzaldehyde (1.041 g, 5 mmol) in dry methanol (20 ml). The mixture was magnetically stirred at room temperature and the course of the reaction was followed by TLC until complete conversion was observed (c.a. 20 h). Then, the remaining mixture was concentrated under vacuum and directly purified by flash column chromatography (5-10 % AcOEt in *n*-hexane) to give the product as a yellow solid (750 mg, 3.68 mmol, 73 %). R_f (10 % AcOEt in *n*-hexane): 0.55. MS

(*z/m*): 204 (M^+ , 100), 203 (100), 202 (100), 189 (77), 165 (32), 101 (39). IR (neat, cm^{-1}): 3271, 3079, 3021, 1508, 1498, 1447, 1412. 1H NMR δ : 7.46-7.32 (6H, mult), 7.26 (2H, mult), 7.17 (1H, tt, $J= 7.4, 1.2$), 7.02 (1H, d, $J= 6.4$), 6.95 (1H, d, $J= 6.4$), 3.03 (1H, s). ^{13}C NMR δ : 137.8, 136.9, 132.4 (x2), 129.8, 128.7 (x2), 127.9, 127.7, 126.6 (x2), 126.3 (x2), 120.6, 83.7, 77.9.

2-((1E,3E,5E,7E)-3,7-dimethyldeca-1,3,5,7-tetraen-9-yn-1-yl)-1,3,3-trimethylcyclohex-1-ene

(Table 1, entry 8). Activated-grade MnO_2 (1.4 g) was placed in a 50 ml round-bottomed flask under nitrogen atmosphere (see before) and darkness, and a dispersion of retinol (250 mg, 0.87 mmol) in *n*-hexane (25 ml) was added. The mixture was magnetically stirred at room temperature and the course of the reaction was followed by TLC until complete conversion was observed (c.a. 2 h 30 min). A new yellow single spot ($R_f= 0.23$ in 10 % AcOEt in *n*-hexane) was observed. Then, dichloromethane (25 ml) was added and the mixture was filtered through a CeliteTM pad. The resulting filtrates were concentrated and the remaining crude was used in the next step without further purification. Dimethyl-1-diazo-2-oxopropylphosphonate (Ohira-Bestmann reagent, 191 mg, 1 mmol) and K_2CO_3 (241 mg, 1.75 mmol) were placed in a 25 ml round-bottomed flask under nitrogen atmosphere (see before) and dry methanol (7 ml) was added. Then, a solution of the obtained crude in dry methanol (3 ml) was added and the mixture was magnetically stirred at room temperature overnight. TLC revealed two new spots (R_f s= 0.69 and 0.45, respectively, in 10 % AcOEt in *n*-hexane). Purification was performed, after concentration of the reaction mixture under vacuum, by flash column chromatography (3-10 % AcOEt in *n*-hexane) to give 45 mg of the topper compound (target product) and 100 mg of the bottom compound (unidentified). R_f (10 % AcOEt in *n*-hexane): 0.69. MS (*z/m*): 280 (M^+ , 83), 265 (36), 209 (57), 195 (66). 1H NMR δ : 6.30-6.00 (5H, mult), 5.38 (1H, dq, $J= 2.5, 1.1$), 3.29 (1H, d, $J= 2.5$), 2.02 (3H, bs), 1.90 (3H, d, $J= 1.1$), 1.64 (3H, t, $J= 0.9$), 1.54 (2H, mult), 1.39 (2H, mult), 1.22 (2H, mult), 0.95 (6H, s).

3.3 XPS

3.4 H/D exchange

-
- ¹ Wilhite, B. A.; McCready, M. J.; Varma, A. *Industrial & Engineering Chemistry Research*. **2002**, *41*, 3345-3350.
- ² Bond, G. B. *Metal-Catalysed Reactions of Hydrocarbons*; Springer.; 2005.
- ³ Dhakshinamoorthy, A.; Pitchumani, K. *Tet. Lett.*. **2008**, *49*, 1818-1823.
- ⁴ Bautista, F. M.; Campelo, J. M.; Garcia, A.; Luna, D.; Quiros, R. A.; Romero, A. A. *Catal. Lett.* **1998**, *52*, 205-213.
- ⁵ Abello, S.; Verboekend, D.; Bridier, B.; Perezramirez, J. J. *J. Catal.* **2008**, *259*, 85-95.
- ⁶ Okamoto, Y.; Nitta, Y.; Toshinobu, I.; Teranishi, S. *J. Catal.* **1980**, *64*, 397-404.
- ⁷ For a review, see Von Schnering, H. G.; Hoenle, W. *Chem. Rev.* **1988**, *88*, 243-273.
- ⁸ Bekaert, E.; Bernardi, J.; Boyanov, S.; Monconduit, L.; Doublet, M.-L.; Ménétrier, M. *J. Phys. Chem. C*. **2008**, *112*, 20481-20490.
- ⁹ Stinner, C.; Tang, Z.; Haouas, M.; Weber, T.; Prins, R. *J. Catal.* **2002**, *208*, 456-466.
- ¹⁰ Sweeny, N.; Rohrer, C.; Brown, O. *J. Am. Chem. Soc.* **1958**, *80*, 799-800.
- ¹¹ For a review, see Oyama, S. T.; Gott, T.; Zhao, H.; Lee, Y.-K. *Catalysis Today*. **2009**, *143*, 94-107.
- ¹² Nelson, A.; Sun, M.; Junaid, A. *J. Catal.* **2006**, *241*, 180-188.
- ¹³ Oyama, S.; Lee, Y. *J. Catal.* **2008**, *258*, 393-400.
- ¹⁴ Li, X.; Zhang, Y.; Wang, A.; Wang, Y.; Hu, Y. *Cat. Commun.* **2010**, *11*, 1129-1132.
- ¹⁵ Carencó, S.; Resa, I.; Le Goff, X.; Le Floch, P.; Mézailles, N. *Chem. Commun.* **2008**, 2568-70.

¹⁶ See for instance: (a) Pachón, L. D.; Rothenberg, G. *Appl. Organomet. Chem.* **2008**, *22*, 288-299; (b) Chen, J.-S.; Vasiliev, A. N.; Panarello, A. P.; Khinast, J. G. *Applied Catalysis A: General.* **2007**, *325*, 76-86; (c) Soomro, S. S.; Ansari, F. L.; Chatziapostolou, K.; Köhler, K. *J. Catal.* **2010**, *273*, 138-146.

¹⁷ Brown, C. A.; Coleman, R. A. *J. Org. Chem.* **1979**, *44*, *13*, 2328-2329.

¹⁸ Note that this second reaction is in agreement with an early report by N. Sweeny *et al.* about the conversion of nitrobenzene to aminobenzene that was achieved in much stronger conditions (*ca* 375°). See reference 10.

¹⁹ Carencó, S.; Boissière, C.; Nicole, L.; Sanchez, C.; Le Floch, P.; Mézailles, N. *Chem. Mater.* **2010**, *22*, 1340-1349.

²⁰ Carencó, S.; Le Goff X.; Shi, J.; Roiban, L.; Ersen, O.; Boissière, C.; Sanchez, C.; Mézailles, N., *Chem. Mater.* **2011**, DOI : 10.1021/cm200575g

²¹ Chiang, R.-K.; Chiang, R.-T. *Inorg. Chem.* **2007**, *46*, 369-71.

²² Leyva, A.; Zhang, X.; Corma, A. *Chem. Commun.* **2009**, *33*, 4897-5044.

²³ Ishizone, T.; Uehara, G.; Hirao, A.; Nakahama, S. *Macromolecules* **1998**, *31*, *12*, 3764.

²⁴ Koradin, C.; Dohle, W.; Rodriguez, A. L.; Schmid, B.; Knochel, P. *Tetrahedron* **2003**, *59*, 1571–1587.